Prediction of α-decay chains and cluster radioactivity of $^{300-304}121$ and $^{302-306}122$ isotopes using the double-folding potential

M. Ismail and A. Adel*

Physics Department, Faculty of Science, Cairo University, Giza, Egypt

(Received 3 November 2019; revised manuscript received 10 January 2020; accepted 4 February 2020; published 18 February 2020)

The α- and cluster-decay half-lives for the two superheavy nuclei (SHN) with $Z = 121$ and 122 have been calculated within the density-dependent cluster model. The α-nucleus potential was constructed by employing the double-folding model with a realistic NN interaction whose exchange part has a finite range. We considered five isotopes for each one of the two SHN, $Z = 121$ and 122, and compared the calculated α-decay half-lives with those obtained from three semiempirical formulas, namely, the Viola-Seaborg-Sobiczewski formula, the modified Brown formula, and the semiempirical formula based on fission theory. The calculated α-decay half-lives are in good agreement with their counterparts. We studied the competition between α-decay and spontaneous fission and predicted possible decay modes for the SHN $^{300-304}121$ and $^{302-306}122$. The cluster decays for $^{300}121$ and $^{302}122$ have been studied within the double folding model, the unified formula, the scaling law of Horoi, and the universal decay law (UDL). We found that the UDL model predicts the possibility of heavy cluster emission from $^{300}121$ and $^{302}122$. We found that the proton and neutron numbers in the emitted clusters and their residual daughter nuclei are magic or near to the magic numbers. We hope that the theoretical prediction of α-decay chains and cluster radioactivity could be helpful for future investigation in this field.

DOI: 10.1103/PhysRevC.101.024607

I. INTRODUCTION

The study of the superheavy nuclei (SHN) has received considerable attention in recent years [1–12]. The rapid development of modern accelerators and detectors facilitates the synthesis of superheavy elements (SHEs) [8,9]. The synthesis of SHEs up to $Z = 113$ (Nh) have been produced based on the closed shell target nuclei of lead and bismuth in the cold fusion reactions [12–15]. The hot fusion reactions involving the fusion of the doubly magic neutron rich ^{48}Ca ions with actinide targets [9,16] lead to neutron rich SHN with much longer half-lives. The heaviest element so far produced is $^{294}_{118}$Og (with a half-life of $0.89^{+1.07}_{-0.31}$ ms) using the $3n$-evaporation channel of the $^{48}\mathrm{Ca} + {}^{249}\mathrm{Cf}$ hot fusion reaction at JINR-FLNR Dubna [17]. The search for even heavier elements is in progress which will be a great challenge [9]. There are significant experimental restrictions on the extension of nuclear landscape to the $Z > 120$ region like limited beam intensities, availability of targets, and long measuring times at cross-section levels of picobarn and below [18]. In such a situation, theoretical predictions became the only tool to investigate such limits.

Superheavy nuclei predominantly undergo consecutive α-decay chains that usually terminated by the spontaneous fission (SF) [9]. Understanding the competition between α decay and spontaneous fission in SHN has become of major importance. Various successful theoretical approaches towards the description of α decay from heavy and SHN have been developed such as the density-dependent cluster model [19–21], the generalized liquid-drop model [22], the coupled channel approach [23,24], the fission-like model [25], the Coulomb and Proximity potential model (CPPM) [26–31]. Several attempts to develop empirical formulas are proposed to predict α-decay half-lives, such as the Viola-Seaborg-Sobiczewski (VSS) formula [32,33], the modified Brown formula (mB1) [34], the semiempirical formula based on fission theory (SemFIS2) [35], the Royer formula [36], the Horoi formula [37], and the universal decay law (UDL) [38]. Recently, we have investigated the competition between α-decay and spontaneous fission for $^{290-298}_{118}$Og and studied the α-decay chains for these isotopes [7]. Saxena *et al.* [39] have performed a systematic study of the structural properties and the decay modes of the SHEs with $Z = 122$, 120, and 118 using the relativistic mean-field plus BCS approach. Within the Coulomb and proximity potential model for deformed nuclei (CPPMDN), Manjunatha studied the α decay properties of superheavy nuclei with $Z = 126$ in the range $288 \leqslant A \leqslant 339$ [40]. Santhosh *et al.* [41] studied the feasibility of observing the α-decay chains from isotopes of SHN with $Z = 128$, 126, 124, and 122 based on the CPPMDN. Qian and Ren have combined the modified two-potential approach with the double folding α-core potential to investigate the α-decay process of heavy and SHN [42].

In the present work, we study the competition between α-decay half-lives and spontaneous fission for the α-decay chains of $^{300-304}121$ and $^{302-306}122$ isotopes which could be useful for the future experiments. The density-dependent

*ahmedadel@sci.cu.edu.eg

cluster model has been adopted in our calculations of the α-decay half-lives. The α-daughter interaction potential is calculated by employing the well-known double-folding model with a realistic M3Y-Paris NN interaction whose exchange part has a finite range. The Q_α values are extracted from the recent reliable Weizsäcker-Skyrme-4 (WS4+) mass model together with the radial basis function (RBF) corrections [43]. The α-particle preformation factor has been calculated using the cluster formation model (CFM) based on the differences in the binding energy [44–47]. The probable cluster decay half-lives from $^{300}121$ and $^{302}122$ are studied within the double folding model, the unified formula (UF) [48], the Horoi scaling law (Horoi) [37], and the universal decay law (UDL) [38].

This article is organized as follows. In Sec. II, we present the theoretical framework for computing the interaction potential between the α or cluster and daughter nuclei. The theoretical models used in the calculation of the α- and cluster decay half-lives are also presented. In Sec. III, the calculated results are discussed. Finally, Sec. IV is devoted to Summary and Conclusion.

II. THEORETICAL FRAMEWORK

A. The α-daughter interaction potential

The α-daughter interaction potential consists of Coulomb (V_C), nuclear (V_N), and centrifugal potentials as [19,49–51]

$$V_{\rm T}(R) = \lambda\, V_N(R) + V_C(R) + \frac{\hbar^2}{2\,\mu}\frac{\left(\ell+\frac{1}{2}\right)^2}{R^2}, \tag{1}$$

where λ represents the renormalization factor of the nuclear potential. It is not a free parameter but it is determined, for decay, by applying the Bohr-Sommerfeld quantization condition [49,52]. R is the separation distance between the mass centers of the α particle and the core. ℓ is the angular momentum carried by the α particle. The last term in Eq. (1) represents the centrifugal potential with the Langer correction [49,52,53], $\ell(\ell+1) \to (\ell+1/2)^2$, which is essential for the validity of the first-order WKB integral [52]. μ is the reduced mass of the α-daughter system.

The nuclear potential $V_N(R)$ composed of two parts, the direct $V_D(R)$ and the exchange $V_{\rm Ex}(R)$ terms, which are given by [54,55]

$$V_D(R) = \int d\vec{r}_1 \int d\vec{r}_2\; \rho_\alpha(\vec{r}_1)\, \upsilon_D(s)\, \rho_d(\vec{r}_2), \tag{2}$$

$$V_{\rm Ex}(R) = \int d\vec{r}_1 \int d\vec{r}_2\; \rho_\alpha(\vec{r}_1, \vec{r}_1+\vec{s})\, \rho_d(\vec{r}_2, \vec{r}_2-\vec{s}) \times \upsilon_{\rm Ex}(s) \exp\left[\frac{i\,\vec{k}(R)\cdot\vec{s}}{M}\right], \tag{3}$$

where s is the NN separation vector. $\rho_\alpha(\vec{r}_1)$ and $\rho_d(\vec{r}_2)$ are the density distributions of the α particle and the daughter nucleus, respectively, and $M = A_1\,A_2/(A_1+A_2)$. The relative-motion momentum $k(r)$ is given by $k^2(r) = 2\,\mu\,[E_{\rm c.m.} - V_N(r) - V_C(r)]/\hbar^2$. $E_{\rm c.m.}$ represents the center-of-mass energy.

The Coulomb potential can be calculated, similar to Eq. (2), within the double folding model in terms of the proton-proton Coulomb interaction (e^2/s) and the involved proton densities as

$$V_C(r) = \iint \rho_{p\alpha}(\vec{r}_1)\, \upsilon_C(s)\, \rho_{pd}(\vec{r}_2) d\vec{r}_1 d\vec{r}_2. \tag{4}$$

The realistic M3Y-Paris NN interaction is used in our calculations and it has the form [54,56]

$$\upsilon_D(s) = \left[11061.625\,\frac{e^{-4s}}{4\,s} - 2537.5\,\frac{e^{-2.5s}}{2.5\,s}\right], \tag{5}$$

$$\upsilon_{\rm Ex}(s) = \left[-1524.25\,\frac{e^{-4s}}{4\,s} - 518.75\,\frac{e^{-2.5s}}{2.5\,s} - 7.8474\,\frac{e^{-0.7072s}}{0.7072\,s}\right]. \tag{6}$$

It is worthy of mention that the folded potential is nonlocal through its exchange term which involves a self-consistency problem because the relative-motion momentum, $k(R)$, depends upon the total nuclear potential, $V_N(R) = V_D(R) + V_{Ex}(R)$, itself. This problem could be solved by the iteration method. More details regarding calculations of the interaction potential within the framework of the double-folding potential can be found in [7,55].

B. α-decay half-lives

The α-decay half-lifetime, $T_{1/2}$, of the parent nucleus is related to the α-decay width, Γ, as

$$T_{1/2} = \frac{\hbar\,\ln 2}{\Gamma}. \tag{7}$$

The calculation of the α-decay width involves the product of three quantities: the penetration probability (P_α), the knocking or assault frequency (ν), and finally the preformation probability (or the so-called spectroscopic factor) of the α-particle inside the parent nucleus (S_α), $\Gamma = \hbar\, S_\alpha\, \nu\, P_\alpha$.

The penetration probability is computed within the framework of the WKB approximation as [19,52]

$$P_\alpha = \exp\left(-2\int_{R_2}^{R_3} dr \sqrt{\frac{2\,\mu}{\hbar^2}\,|V_T(r) - Q_\alpha|}\right), \tag{8}$$

where the three turning points, R_i ($i = 1, 2, 3$), are obtained from $V_T(r)|_{r=R_i} = Q_\alpha$. Q_α is the Q value of the α decay and μ is the reduced mass.

The assault frequency, ν, is given by [52]

$$\nu = T^{-1} = \frac{\hbar}{2\,\mu}\left[\int_{R_1}^{R_2} \frac{dr}{\sqrt{\frac{2\,\mu}{\hbar^2}\,|V_T(r) - Q_\alpha|}}\right]^{-1}. \tag{9}$$

The α particle is assumed to exist on the surface of the parent nucleus with a definite preformation probability, before its emission. In the present calculations, the preformation factor S_α is calculated using the reliable cluster formation model (CFM) based on the differences in the binding energy [47].

We have compared our calculations of α-decay half-lives using the double-folding potential with the following three semiempirical formulas and with the spontaneous-fission half-lives which will be briefly described below.

1. The Viola-Seaborg semiempirical formula (VSS)

One of the commonly used formulas in calculating α-decay half-lives is the Viola-Seaborg semiempirical (VSS) formula which proposed by Viola and Seaborg [32] with constants determined by Sobiczewski *et al.* [33],

$$\log_{10}\left(T_{1/2}^{\rm VSS}\right) = (aZ+b)\,Q^{-1/2} + c\,Z + d + h_{\log}, \qquad (10)$$

where Z is the atomic number of the parent nucleus and the half-life $T_{1/2}$ is in seconds, the Q value is in MeV. The constants a, b, c, and d are adjustable parameters obtained through a least-square fit to even-even nuclei and the quantity $h_{\log}$ represents the hindrance factor for nuclei with unpaired nucleons. The constants are $a = 1.66175$, $b = -8.5166$, $c = -0.20228$, $d = -33.9069$, and

$$h_{\log} = \begin{cases} 0 & \text{for } Z, N \text{ even}, \\ 0.772 & \text{for } Z = \text{odd}, N = \text{even}, \\ 1.066 & \text{for } Z = \text{even}, N = \text{odd}, \\ 1.114 & \text{for } Z, N \text{ odd}. \end{cases}$$

2. Modified Brown formula (mB1)

Another formula used in present work is the modified Brown (mB1) formula with an additional hindrance term depending on parity [34]

$$\log_{10}\left(T_{1/2}^{\rm mB1}\right) = a(Z-2)^b\,Q^{-1/2} + c + h^{\rm mB1}. \qquad (11)$$

The constants are $a = 13.0705$, $b = 0.5182$, $c = -47.8867$, and

$$h^{\rm mB1} = \begin{cases} 0 & \text{for } Z, N \text{ even}, \\ 0.6001 & \text{for } Z = \text{odd}, N = \text{even}, \\ 0.4666 & \text{for } Z = \text{even}, N = \text{odd}, \\ 0.8200 & \text{for } Z, N \text{ odd}. \end{cases}$$

3. Semiempirical formula based on fission theory (SemFIS2)

Poenaru *et al.* [35] proposed semiempirical formula for α-decay half-lives based on fission theory (SemFIS2) which is expressed as

$$\log_{10}\left(T_{1/2}^{\rm SemFIS2}\right) = 0.43429\,\chi(x,y)\cdot K - 20.446 + H^f, \qquad (12)$$

where

$$K = 2.52956\,Z_d[A_d/(A\,Q)]^{1/2}[\arccos\sqrt{r} - \sqrt{r(1-r)}], \qquad (13)$$

and $r = 0.423\,Q(1.5874 + A_d^{1/3})/Z_d$. The numerical coefficient χ, close to unity, is a second order polynomial:

$$\chi(x,y) = B_1 + x\,(B_2 + x\,B_4) + y\,(B_3 + y\,B_6) + x\,y\,B_5. \qquad (14)$$

In Ref. [35], the following set of parameter values are obtained for transuranium nuclei $B_1 = 0.985415$, $B_2 = 0.102199$, $B_3 = -0.024863$, $B_4 = -0.832081$, $B_5 = 1.50572$, and $B_6 = -0.681221$. The hindrance factor H^f takes different values $H^f_{ee} = 0$ for even-even emitters, $H^f_{eo} = 0.63$, $H^f_{oe} = 0.51$, and $H^f_{oo} = 1.26$. The reduced variables x and y are defined as

$$x \equiv (N - N_i)/(N_{i+1} - N_i); \quad N_i < N \leqslant N_{i+1}, \qquad (15)$$

$$y \equiv (Z - Z_i)/(Z_{i+1} - Z_i); \quad Z_i < Z \leqslant Z_{i+1} \qquad (16)$$

with $N_i = \ldots, 51, 83, 127, 185, 229, \ldots, Z_i = \ldots, 29, 51, 83, 127, \ldots$, hence for the region of superheavy nuclei $x = (N - 127)/(185 - 127)$, $y = (Z - 83)/(127 - 83)$.

4. Spontaneous fission half-lives

The spontaneous fission is the other competing mode to α decay in the superheavy region. To identify the decay mode of SHN, the spontaneous-fission half-lives were evaluated using the semiempirical formula given by Xu *et al.* [57]

$$T_{1/2} = \exp\left\{2\pi\left[C_0 + C_1 A + C_2 Z^2 + C_3 Z^4 + C_4 (N-Z)^2 - \left(0.13323\frac{Z^2}{A^{1/3}} - 11.64\right)\right]\right\}. \qquad (17)$$

The constants are $C_0 = -195.09227$, $C_1 = 3.10156$, $C_2 = -0.04386$, $C_3 = 1.4030 \times 10^{-6}$, and $C_4 = -0.03199$.

C. The cluster-core system within the density-dependent cluster model

The ground state of the parent nucleus can be visualized as a two-body system involving a cluster interacting with a daughter nucleus. The interaction potential of cluster-daughter system is a sum of attractive nuclear $V_N(R)$, the repulsive Coulomb $V_C(R)$ potentials, and the centrifugal part similar to Eq. (1).

The Bohr-Sommerfeld quantization condition [49] is used to determine the renormalization factor λ of the nuclear potential, Eq. (1), as

$$\int_{R_1}^{R_2} dr\sqrt{2\,\mu|V_T(r) - Q_c|/\hbar^2} = (2n+1)\frac{\pi}{2} = (G - \ell + 1)\frac{\pi}{2}, \qquad (18)$$

where the three turning points R_i $(i = 1, 2, 3)$ (fm) for the cluster-daughter potential barrier are defined by the equation $V_T(r)|_{r=R_i} = Q_c$. The released energy for the cluster decay, Q_c, is extracted using the recent mass model WS4+ together with the radial basis function (RBF) corrections [43]. The quantum number n is chosen according to the Wildermuth and Tang condition [58,59],

$$G = 2n + \ell = \sum_{i=1}^{A_c}\left(g_i^{(A_c+A_d)} - g_i^{(A_c)}\right), \qquad (19)$$

where $A_c(A_d)$ is the mass number of the emitted cluster (daughter nucleus) and $g_i^{(A_c+A_d)}$ are the oscillator quantum numbers of the nucleons belonging to the cluster inside the parent nucleus, whose values are required to ensure the cluster completely outside the shell occupied by the core nucleus, and $g_i^{(A_c)}$ are the internal quantum numbers of the A_c nucleons in the individual emitted cluster [60,61]. Here, we take $g_i(50 \leqslant Z, N \leqslant 82) = 4$, $g_i(82 < Z, N \leqslant 126) = 5$, $g_i(126 < N \leqslant 184) = 6$, and $g_i(N > 184) = 7$, where Z and N are the proton and neutron number of the daughter nucleus [60,61].

The cluster decay half-life is related to the cluster decay width Γ_c and the cluster preformation probability S_c as [62,63]

$$T_{1/2} = \frac{\hbar \ln 2}{S_c\, \Gamma_c}, \tag{20}$$

The cluster decay width is defined as $\Gamma_c = \hbar\, \nu_c\, P_c$. Here, ν_c, and P_c are the knocking frequency and barrier penetrability of the emitted cluster, respectively. By applying the Wentzel-Kramers-Brillouin (WKB) approximation, one can express the ν_c, and P_c as [61,63]

$$\nu_c = \left[\int_{R_1}^{R_2} \frac{2\,\mu}{\hbar \sqrt{2\,\mu\, |V_T(r) - Q|/\hbar^2}}\, dr \right]^{-1} \tag{21}$$

and

$$P_c = \exp\left(-2 \int_{R_2}^{R_3} \sqrt{2\,\mu\, |V_T(r) - Q|/\hbar^2}\, dr \right). \tag{22}$$

In the present calculations, the cluster preformation probability, S_c, can be expressed using the following formula [59,60]:

$$\log_{10} S_c = a \sqrt{\mu\, Z_c\, Z_d} + b, \tag{23}$$

where $Z_c(Z_d)$ is the atomic number of the emitted cluster (daughter nucleus). The parameters a and b of the formula given by Eq. (23) are obtained from Ref. [60] with the values $a = -0.052$, $b_{e-e} = 0.690$, and $b_{o-A} = -0.600$.

III. RESULTS AND DISCUSSIONS

In the present work, we have used the density-dependent cluster model with the microscopic α-nucleus potential derived from the double-folding model to calculate the α-decay half-lives ($T_{1/2}$) for five isotopes of each of the two SHN with $Z = 121$ and 122 and their corresponding decay products. The α-particle preformation factors needed for the calculations by this method are extracted from cluster formation model given in Ref. [47]. The half-lives calculated by this method are denoted by $T_{1/2}^{\text{calc.}}$. The α-decay half-lives are also calculated using the three semiempirical formulas given by Eqs. (10), (11), and (12). The half-lives calculated from these equations are denoted by $T_{1/2}^{\text{VSS}}$, $T_{1/2}^{\text{mB1}}$, and $T_{1/2}^{\text{SemFIS2}}$, respectively. All the above calculations assume spherical shapes for the daughter nuclei and have performed using Q_α values extracted from the recent WS4+ mass model [43]. It should be noted that the WS4+ mass model is one of the most reliable mass models for the study of Q_α values of SHN, it has an accuracy smaller than 300 keV [43].

For SHN, the most important decay modes are the emission of α-particle and spontaneous fission (SF). The identification of the isotopes of new superheavy elements possess a problem because their α-decay chains terminates by SF before reaching the known region of nuclear chart. Therefore, the theoretical predictions about the stability of the isotopes of SHEs against α decay, SF, and the competition between them are useful in interpreting the experimental results. In the present work, the spontaneous fission half-lives T_{SF} have been calculated using the semiempirical formula given by Eq. (17), developed by Xu *et al.* [57].

It is worthy of mention that the Pauli principle forbids the nucleons in the cluster from occupying the same states as the nucleons in the core. The major requirements of the Pauli principle are approximately satisfied through the Wildermuth-Tang (WT) rule by restricting the quantum numbers of relative motion to values which ensure that the constituent nucleons of the α particle occupy states immediately above the Fermi surface of the daughter (core) nucleus. This is sufficient to account for the main effects of the Pauli principle, and the remaining effects are largely incorporated into the effective α-nucleus potential via the knock-on exchange contribution which guarantees the antisymmetrization of identical nucleons in the α cluster and the daughter nucleus [64]. A proper normalization of the α-daughter nuclear potential is performed through the Bohr-Sommerfeld (BS) quantization condition, which fulfills the periodicity of particle motion. Therefore, the quasibound states of an α cluster can be defined approximately by the Bohr-Sommerfeld quantization condition, and a link to the shell model can be obtained with the Wildermuth rule [65]. Several forms of the nuclear part of the α-core potential have been successfully employed in earlier works [64–67] to satisfactorily describe α-decay half-lives by imposing the WT prescription such as the Woods-Saxon (WS) potential [66], the so-called Cosh potential [67], the modified Woods-Saxon (WS + WS^3) potential [68,69], the double-folding potential [64,66,70–73], and the Skyrme energy-density functional potential [65,74]. The nucleus-nucleus interaction derived from the Skyrme nucleon-nucleon force has a hard core followed by a pocket [74], the α particle in this case cannot move in the internal region. On the other hand, the effective nucleon-nucleon M3Y-Paris within the double-folding model generates the nucleus-nucleus potential with repulsive direct part and strong attractive exchange contribution. The sum of the two contributions is attractive and has almost the Woods-Saxon shape [66]. The total α-daughter potential, given by Eq. (1), has hard core near the center with too small radius due to existence of centrifugal part. Thus, the almost Woods-Saxon shape of nuclear part and the hard core with two small radius permit the application of the BS quantization condition along with the WT prescription for the adopted double-folding potential, which simulates the Pauli principle.

Figure 1 depicts the variation of $\log_{10}(T_{1/2}^{\text{calc.}}/T_{1/2}^{\text{expt.}})$ for the recently synthesized SHN [10] as a function of the neutron number N_p of the parent nucleus. To quantify the accuracy of our α-decay calculations in the superheavy region, we have computed the standard deviation, σ, for the logarithmic half-lives between the experimental and calculated values using the following equation:

$$\sigma = \left[\frac{1}{n-1} \sum_{i=1}^{n} \left(\log_{10} T_{1/2}^{\text{calc.}} - \log_{10} T_{1/2}^{\text{expt.}} \right)^2 \right]^{1/2}. \tag{24}$$

The standard deviation of the logarithmic half-life is found to be 0.563 for the calculations of $T_{1/2}^{\text{calc.}}$ for the recently synthesized SHN [10]. As can be seen from Fig. 1 that most of the points lie near $\log_{10}(T_{1/2}^{\text{calc.}}/T_{1/2}^{\text{expt.}}) = 0$. This means that the calculated α-decay half-lives are in good agreement with the experimental data for the measured SHN and we

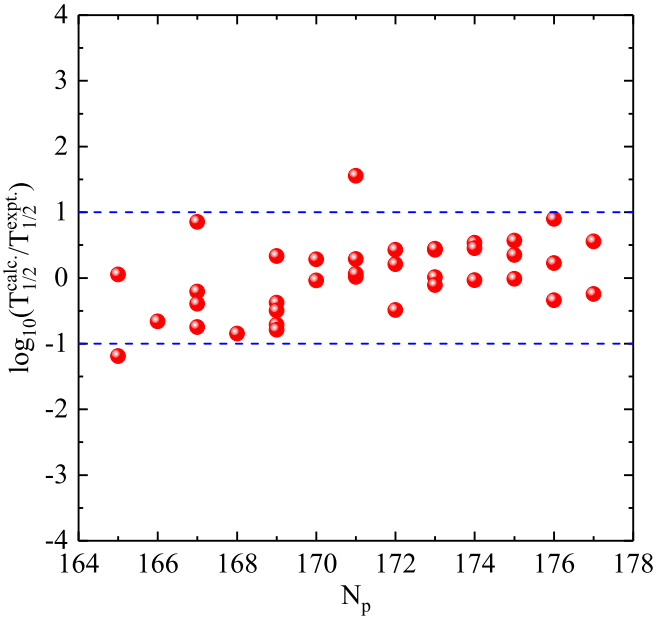

FIG. 1. Deviation of the calculated α-decay half-lives, using S_α derived from the cluster formation model [47], with the corresponding experimental half-lives for the recently synthesized SHN [10].

can extend our calculations to predict the α-decay half-lives for the unknown isotopes of the superheavy elements with $Z = 121$ and 122.

Figure 2 shows the comparison between the four α-decay half-lives $T_{1/2}^{\text{Calc.}}$, $T_{1/2}^{\text{VSS}}$, $T_{1/2}^{\text{mB1}}$, and $T_{1/2}^{\text{SemFIS2}}$ and the SF half-lives, T_{SF}, for the five isotopes $^{300\text{–}304}121$ and their α-decay products. Figure 3 is the same as Fig. 2 but for the five isotopes $^{302\text{–}306}122$ and their α-decay products. Figure (a) displays our results for the isotope $^{300}121$ and its α-decay chains. Figure 2(a) shows that the elements $^{300}121$, $^{296}119$, $^{292}117$, and $^{288}115$ have α-decay half-lives less than the corresponding T_{SF}. Thus, the isotope $^{300}121$ survives fission and our study predicts 4-α chains from this isotope. Figures 2(b), 2(c), 2(d), and 2(e) show that the isotopes $^{301}121$, $^{302}121$, $^{303}121$, and $^{304}121$ survive fission and the present study predicts 4-α chains from $^{301}121$, and 3-α chains from each of the three other isotopes. Figure 3 shows the results for the isotopes of the SHE $Z = 122$ and their α-decay chains. Figure 3(a) shows that the isotope $^{302}122$ survives fission and 4-α chains are expected from this isotope. Calculations using mB1 predicts 5-α chains from the isotope $^{302}122$. Figures 3(b), 3(c), and 3(d) show that the isotopes $^{303}122$, $^{304}122$, and $^{305}122$ survive fission and 4-α chains are predicted from each isotope. Figure 3(e) displays the results for the isotope $^{306}122$. Figure 3(e) show that the α-decay half-life calculated using the double-folding model, $T_{1/2}^{\text{calc.}}$, for the element $^{294}116$ is larger than T_{SF}, $T_{1/2}^{\text{VSS}}$, $T_{1/2}^{\text{mB1}}$, and $T_{1/2}^{\text{SemFIS2}}$ are smaller than T_{SF}. For the elements $^{306}122$, $^{302}120$, $^{298}118$, all α-decay half-life times are smaller than T_{SF}. Thus the isotope $^{306}122$ survives fission and we predict 4-α chains from this isotope when the α-decay half-lives are calculated using VSS, mB1, and SemFIS2 models. We predict 3-α chains from this isotope when the half-life is calculated using the folding model.

It is known that the behavior of the α-decay half-life times of the isotopes of the SHEs $Z = 121$ and 122 and their corresponding decay products as the mass number of the parent nucleus A_p decreases is governed by the existence of neutron and/or proton magic or semimagic numbers. At magic or nucleon stability numbers, the nucleus becomes more stable against α decay and $T_{1/2}$ becomes large. The microscopic shell correction with the traditional Strutinsky procedure are taken into account in the present calculations through the WS4+ mass model from which the Q_α values, used in the present calculations, are extracted. Thus the shell effects are implicitly incorporated in the Q_α values and govern the behavior of T_α with mass number variation. The maxima in Figs. 2(a)–2(e) occur at proton and neutron numbers of the parent nuclei at $(Z_p, N_p) = (113, 171)$, (113,172), (113,173), (111,172), and (111,173), respectively. The proton number $Z = 113$ differs by only one from the proton magicity $Z = 114$ [75–77], also the neutron number in the brackets differ by one or equal to the neutron magicity $N = 172$ [75,76]. In Fig. 2(d), the maximum value of $T_{1/2}$ at (111,172) has almost the same value of $T_{1/2}$ as the half-life time $T_{1/2}$ at $(Z_p, N_p) = (113, 174)$. The first bracket (111,172) has Z_p value differs by three from proton magicity and N_p value corresponds to neutron magic number. The second bracket (113,174) has Z_p differs by one from $Z = 114$ and N_p differs by two from $N = 172$. The minima in the Figs. 2(a)–2(e) occur at $(Z_p, N_p) = (109, 167)$, (109,168), (109,169), (109,170), and (109,171), respectively. The value $Z_p = 109$ is far from the nearest proton magicity. The highest point (corresponding to the largest T_α) in each of the five figures have $(Z_p, N_p) = (103, 161)$, (103,162), (103,163), (103,164), and (103,165). $Z_p = 103$ is near the proton magicity $Z = 102$ found in Refs. [75–77], also N_p has value near the neutron magicity $N = 160$ and 162.

Figure 3 is similar to Fig. 2 but for the SHE with $Z = 122$. A clear maximum appears in Fig. 3(a) at the double magic numbers $(Z_p, N_p) = (114, 172)$. As the number of neutrons increases at $Z_p = 114$, the neutron number in the nucleus becomes far from magicity and the maximum becomes less clear, as in Figs. 3(b) and 3(c), then the maximum at the proton magic number $Z_p = 114$ disappears as in Figs. 3(d) and 3(e). The minima in the Figs. 3(a)–3(e) occur at $Z_p = 110$ or 108 with neutron number $N_p = 168$, 169, and 170.

The largest $T_{1/2}$ in the Figs. 3(a)–3(e) correspond to $Z_p = 104$ and $N_p = 162$, 163, 164, 165, and 166. $Z = 104$ is near the proton magicity $Z = 102$ and $N_p = 162$ is a neutron magicity. Also, $N_p = 164$ corresponding to filling the neutron level $1j_{15/2}$ in studying the single particle spectrum of the double closed shell $^{298}114$ nucleus [75–77]. Thus, $N_p = 164$ can be considered as a semi neutron magic number (large energy gap exists between this level and the next one).

Figure 4(a) illustrates the logarithm of the ratio of the calculated α-decay half-lives from different approaches to the calculated values from our adopted model as a function of the parent neutron number for the α-decay chains of $^{300\text{–}304}121$ isotopes. Figure 4(b) is similar to Fig. 4(a) but for the α-decay chains of $^{302\text{–}306}122$ isotopes. It is clear from Figs. 4(a) and 4(b) that the calculated α-decay half-lives using

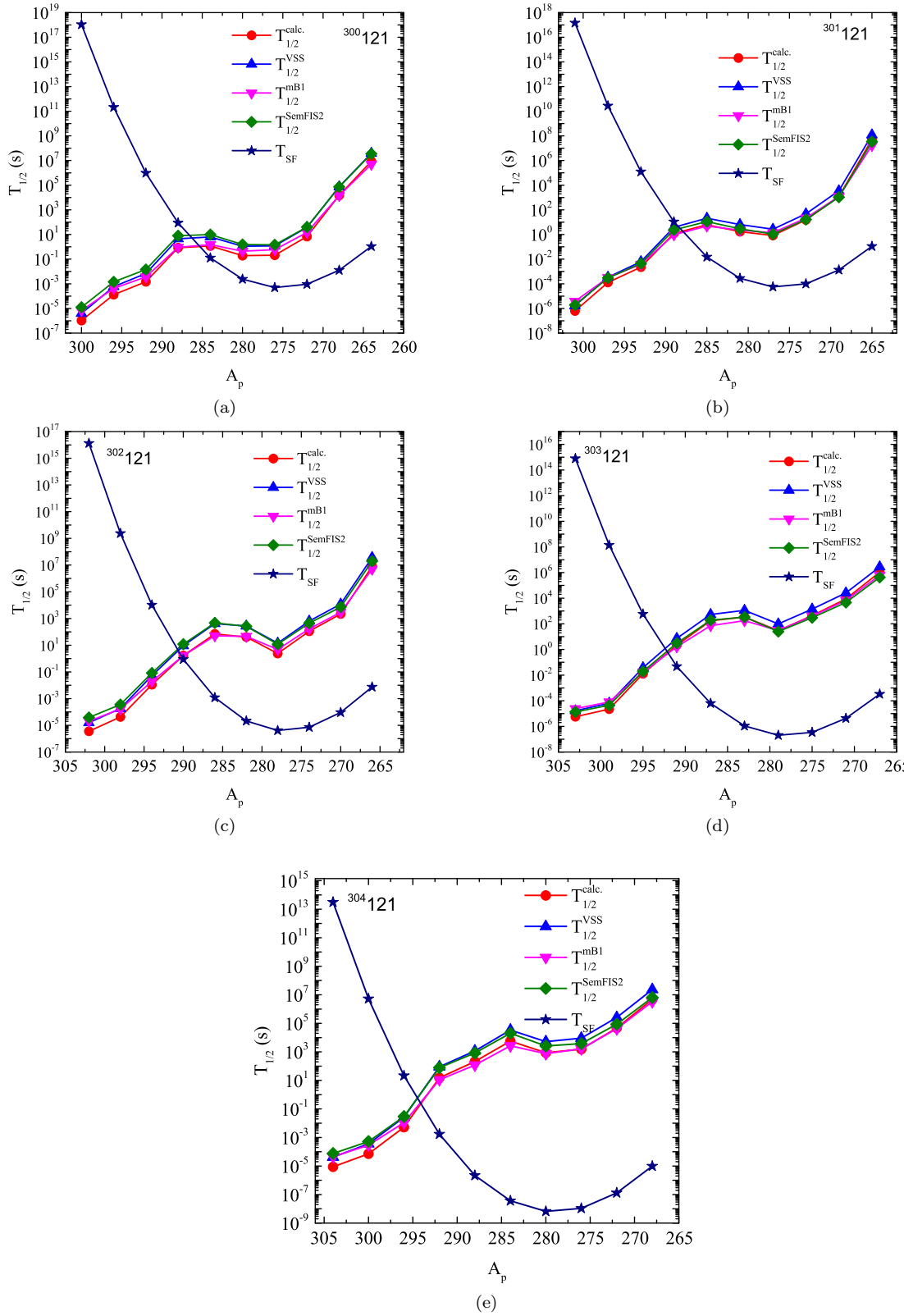

FIG. 2. Comparison of the calculated α-decay half-lives of the isotopes with $Z = 121$ and products on its α-decay chain.

our adopted model are in satisfactory agreement with their counterparts from other theoretical approaches. The standard deviation, σ, for the logarithmic half-lives between different approaches and our calculated values for the α-decay chains of $^{300-304}121$ isotopes are, respectively, 0.642, 0.356, and 0.625 for VSS, mB1, and SemFIS2. For the α-decay chains of $^{302-306}122$ isotopes, the values of σ are, respectively, 0.492, 0.474, and 0.356 for VSS, mB1, and SemFIS2.

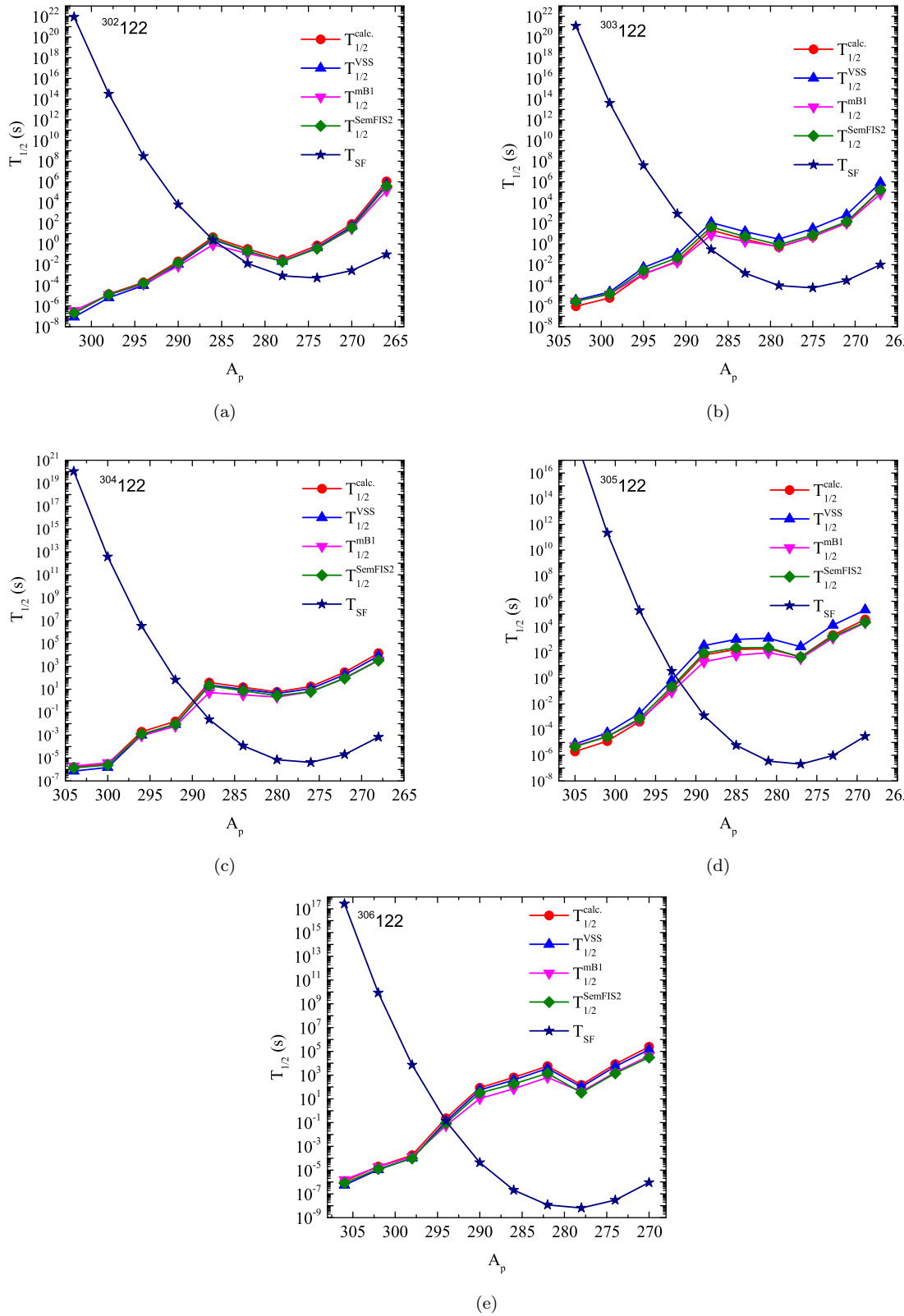

FIG. 3. Comparison of the calculated α-decay half-lives of the isotopes with $Z = 122$ and products on its α-decay chain.

Figure 5(a) shows the logarithm of preformation factor S_α as a function of the fragmentation (or driving) potential, $V_B - Q$, which is defined as the difference between the Coulomb barrier height V_B and the Q value for odd-odd $^{288-342}121$ isotopes. It is clear from Fig. 5(a) that there is a negative linear correlation between the logarithm of S_α and the fragmentation potential. Figure 5(b) which is similar to Fig. 5(a) but for even-even $^{292-342}122$ isotopes shows similar behavior. This

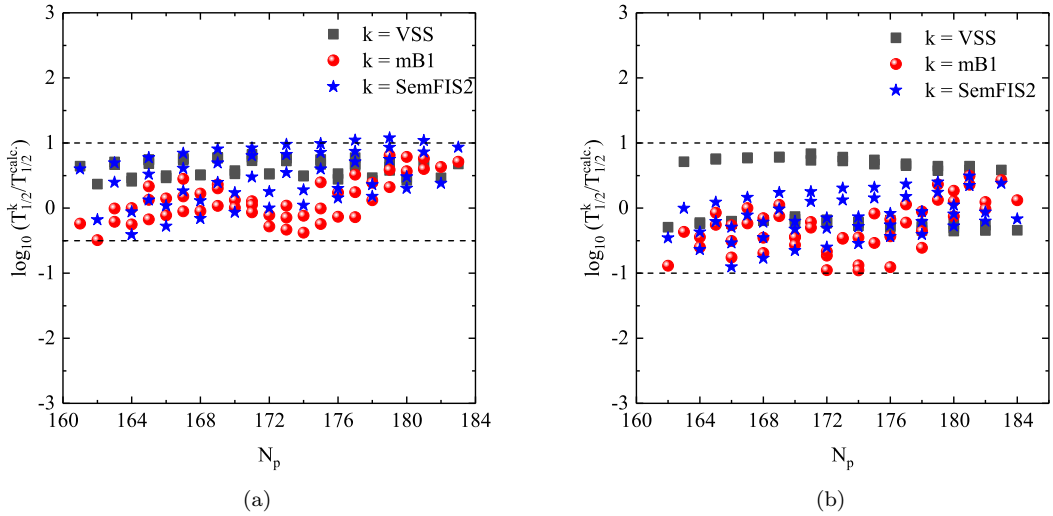

FIG. 4. Deviation of the calculated α-decay half-lives, using S_α derived from the cluster formation model [47], with the corresponding theoretical α-decay half-lives from several approaches for the decay chains of (a) $^{300-304}121$ isotopes and (b) $^{302-306}122$ isotopes.

result supports the conclusion drawn in Ref. [78] in which a universal analytical relation expressing the logarithm of the reduced width squared (proportional to S_α) as a linear function in terms of the fragmentation potential was derived.

Cluster decay is an important decay mode of SHN. Poenaru *et al.* [79,80] predicted that the cluster decay is one of the important decay modes of SHN and its branching ratio could be larger than that of α decay for SHN with $Z \geqslant 121$ when calculated by the superasymmetric fission model or by the universal decay law (UDL) [38]. In the present work, we examine the feasibility of emission of different clusters from $^{300}121$ and $^{302}122$ superheavy nuclei. We use four different models to calculate the cluster decay half-lives. These models are the double folding model with the M3Y-Paris as *NN* interaction and assuming finite-range exchange part [54,55], the unified formula (UF) of the half-lives for α-decay and cluster radioactivity [48], the scaling law by Horoi [37], and the universal decay law (UDL) [38].

Table I shows the α and cluster decay of the two SHN $^{300}121$ and $^{302}122$. The table indicates that $T_{1/2}$ for clusters with mass numbers greater than $A_c = 60$ is greater than 10^{30} s when calculated from UF and Horoi formulas. Calculations using the folding model and the UDL produce cluster decay half-lives $T_{1/2} < 10^{30}$ s. It is noted that the clusters with $T_{1/2} < 10^{30}$ s may be detected through experiments [81]. A good measure of the competition between α decay and cluster radioactivity (CR) is the value of the branching ratio of CR relative to the corresponding α-decay. It is given by $\log b_c = \log T_\alpha - \log T_c$. If $\log b_c > 0$, means that CR is the dominant decay mode against α decay. If $b_c \ll 0$ means that α-decay half-lives are much less than cluster decay half-lives. The predicted half-lives by UDL formula produce positive

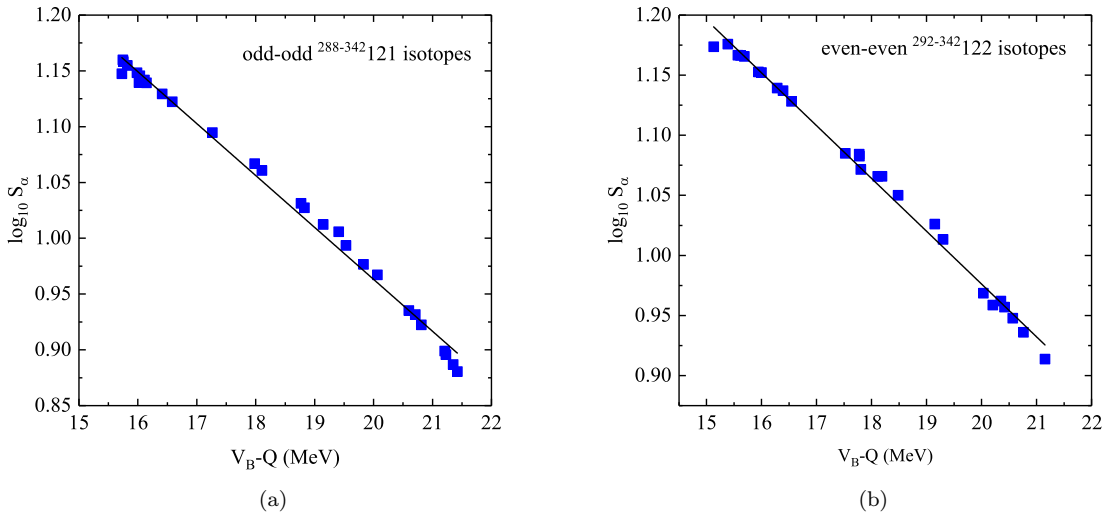

FIG. 5. A negative linear correlation between the logarithm of the α-preformation factor, S_α, and the fragmentation potential (defined as $V_B - Q$) (a) for odd-odd $^{288-342}121$ isotopes (b) for even-even $^{292-342}122$ isotopes.

TABLE I. The probable cluster decay half-lives of $^{300}121$ and $^{302}122$ within the double-folding model based on M3Y-Paris *NN* interaction with the finite-range exchange part, (calc.), as well as the unified formula (UF) of half-lives for α decay and cluster radioactivity [48], the scaling law by Horoi [37], (Horoi), and the universal decay law (UDL) [38]. The Q values are extracted from the recent WS4+ mass model [43] (often denoted as WS4 + RBF) are Weizsacker-Skyrme models applying the radial basis function (RBF) approach.

			$\log_{10} T$			
Parent nuclei	Emitted clusters	$Q_c^{\mathrm{WS4+}}$ (MeV)	Calc.	UF	Horoi	UDL
$^{300}121$	^{4}He	13.783	−5.98	−5.49	−5.90	−5.98
	^{16}O	62.318	20.35	23.57	21.34	21.93
	^{28}Mg	105.411	23.12	28.48	28.20	22.13
	^{32}Si	126.768	22.77	28.44	29.40	20.10
	^{68}Ni	249.068	27.70	38.53	48.60	11.73
	^{76}Zn	261.365	29.25	42.12	53.00	11.88
	^{79}Ga	268.684	28.72	42.15	53.81	10.57
	^{80}Ge	278.714	25.94	38.99	52.18	6.69
	^{83}As	286.804	24.43	37.94	52.24	4.33
	^{84}Se	295.952	22.15	35.35	51.01	1.06
	^{85}Br	302.783	21.53	34.64	51.00	−0.27
	^{86}Kr	309.585	–	33.79	50.89	−1.74
	^{89}Rb	317.515	–	32.19	50.57	−4.57
	^{90}Sr	323.966	–	31.30	50.42	−6.04
	^{91}Sr	324.660	–	30.89	50.29	−6.75
	^{92}Sr	324.981	–	30.78	50.36	−7.15
	^{93}Sr	323.062	–	32.55	51.61	−5.64
	^{94}Sr	322.030	–	33.58	52.39	−4.86
	^{96}Y	326.610	–	34.20	53.31	−5.03
	^{96}Zr	332.818	–	32.96	52.78	−6.55
	^{99}Nb	333.352	–	36.73	55.78	−3.72
	^{102}Mo	336.137	–	38.42	57.40	−2.97
$^{302}122$	^{4}He	14.212	−6.72	−5.97	−6.36	−6.49
	^{16}O	64.414	18.45	21.69	19.68	19.89
	^{28}Mg	106.999	22.60	28.00	27.83	21.45
	^{32}Si	129.281	21.60	27.27	28.52	18.67
	^{68}Ni	253.146	26.75	37.63	48.16	10.26
	^{76}Zn	264.943	28.89	41.88	53.04	11.03
	^{79}Ga	269.984	30.37	44.15	55.34	11.99
	^{80}Ge	282.085	25.97	39.19	52.53	6.25
	^{83}As	287.794	26.46	40.38	54.08	6.16
	^{84}Se	298.950	22.66	36.10	51.75	1.14
	^{85}Br	303.932	23.54	37.09	52.84	1.53
	^{86}Kr	312.821	–	34.54	51.64	−1.69
	^{89}Rb	318.259	–	35.14	52.75	−2.29
	^{90}Sr	326.665	–	32.69	51.61	−5.37
	^{91}Sr	325.905	–	33.49	52.25	−4.85
	^{92}Sr	329.097	–	31.01	50.80	−7.69
	^{93}Sr	326.080	–	33.68	52.64	−5.24
	^{94}Sr	326.717	–	33.31	52.53	−5.91
	^{96}Y	327.920	–	36.88	55.33	−3.08
	^{96}Zr	339.573	–	31.20	51.99	−9.16
	^{99}Nb	337.947	–	36.83	56.16	−4.45
	^{102}Mo	343.124	–	36.59	56.59	−5.69

or small negative values of $\log b_c$ for the heavy clusters ^{89}Rb, $^{90-94}$Sr, ^{96}Y, and ^{96}Zr emissions from $^{300}121$ and the heavy clusters $^{90-94}$Sr, ^{96}Zr, and ^{102}Mo emission from $^{302}122$. These clusters are the main decay modes of $^{300}121$ and $^{302}122$ within the UDL model. Let us discuss the protons and neutrons distribution in the emitted clusters. The cluster ^{89}Rb has $(Z, N) = (37, 52)$ and the daughter nucleus has $(Z, N) = (84, 127)$. The clusters $^{90-94}$Sr has proton number $Z = 38$ and the number of neutrons are $N = 52$, 53, 54, 55, and 56 for the mass numbers 90, 91, 92, 93, and 94, respectively. The residual nuclei after Sr emission have $Z = 83$ and the number of neutrons are 127, 128, 129, 130, and 131. The

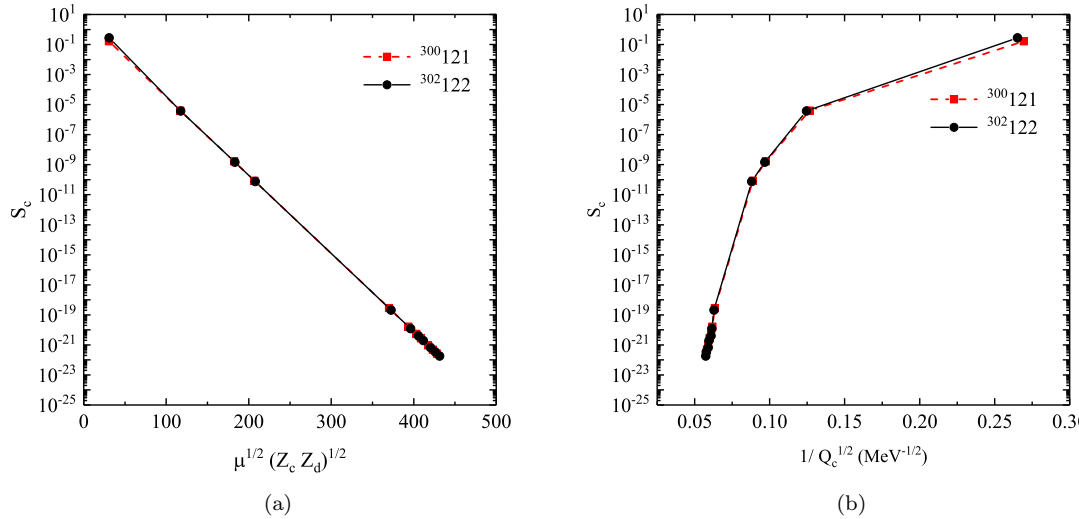

FIG. 6. (a) The variation of the cluster preformation factor, S_c, for different clusters emitted from ^{300}121 and ^{302}122 isotopes as a function of (a) $\mu^{1/2}\,(Z_c\,Z_d)^{1/2}$, (b) $1/\sqrt{Q_c}$.

heavy cluster ^{96}Y has $Z = 39$ and $N = 57$ and its daughter nucleus is the ^{204}Pb element. The cluster ^{96}Zr has $Z = 40$ and $N = 56$, its residual nucleus has $Z = 81$ and $N = 123$. The above neutron and proton numbers in the cluster and daughter nuclei correspond to near magic nucleon numbers. For example, the atomic number Z for the emitted clusters are 37, 38, 39, and 40 which are equal to the proton magic number $Z = 40$ or near this number. Also the neutron numbers in the five clusters $^{90-94}$Sr are near the neutron magicity $N = 50$. The residual daughter have proton numbers in the vicinity of the magic numbers $Z = 82$ and $N = 126$. This means that the SHN with $Z = 121$ tends to emit clusters with nucleon numbers correspond to magic or differ slightly than proton and neutron magic numbers.

The SHN ^{302}122 tends to emit the same Zr and Sr clusters beside ^{102}Mo. The last heavy cluster has $Z = 42$ and $N = 60$ and its residual daughter nucleus has $Z = 80$ and $N = 120$. The atomic number of the cluster differs slightly from the proton magicity $Z = 40$ and $Z = 80$ correspond to completely filled proton levels before the level $3s_{1/2}$ at the top of the closed shell $Z = 82$. Moreover, $N = 120$ corresponds also to completely filled neutron levels before the two levels at the top of the closed shell $N = 126$ as shown on Fig. 1 in Ref. [82].

The preformation probability of cluster depends practically on the sizes of the cluster and the daughter nucleus. Based on this fact, the formula for S_c, Eq. (23), was suggested in [59,60]. Figure 6(a) illustrates the variation of the cluster preformation factor S_c, for the different clusters emitted from ^{300}121 and ^{302}122 isotopes, as a function of the quantity $\mu^{1/2}\,(Z_c\,Z_d)^{1/2}$. It is clear from Fig. 6(a) that the cluster preformation factor decreases considerably in magnitude with increasing the size of the cluster. Figure 6(b) shows the variation of S_c as a function of $1/\sqrt{Q_c}$ for different clusters emitted from ^{300}121 and ^{302}122 nuclei. It is clear from Fig. 6(b) that S_c decreases as the Q-value increases.

IV. SUMMARY AND CONCLUSION

We studied the α-decay chains of five isotopes of the SHN with $Z = 121$ and 122 using the density-dependent cluster model. The α-nucleus potential have been derived within the double-folding model with realistic M3Y-Paris NN interaction and the α-decay half-lives of the isotopes $^{300-304}$121 and $^{302-306}$122 have been calculated. The α-decay preformation factors were derived from the recent cluster formation model. The calculated α-decay half-lives are in satisfactory agreement with the corresponding results obtained from the semiempirical formulas: VSS, mB1, and SemFIS2. Comparison between α-decay and spontaneous fission half-lives predicts 4-α chains from each of the isotopes ^{300}121 and ^{301}121 while 3-α chains are observed from each one of the three isotopes $^{302-304}$121. For the SHN with $Z = 122$, the comparison between these decay modes predicts 5-α chains or 4-α chains from the isotope ^{302}122, 4-α chains from each one of the isotopes $^{303-305}$122, and 3-α chains or 4-α chains from the isotope ^{306}122. We studied the behavior of α-decay half-lives as the mass number of the parent nuclei is varied and found that this behavior is governed by magic and semimagic numbers of protons and neutrons.

We also studied the probable cluster decay radioactivity from ^{300}121 and ^{302}122 within the double folding model, the unified formula (UF) [48], the Horoi scaling law (Horoi) [37], and the universal decay law (UDL) [38]. We found that, within the UDL model, eight heavy cluster emissions are observed from the decay of ^{300}121 and seven clusters could be emitted from ^{302}122 which may be compared to or dominant over α decay. These clusters are ^{89}Rb, $^{90-94}$Sr, ^{96}Y, and ^{96}Zr from ^{300}121 and $^{90-94}$Sr, ^{96}Zr, and ^{102}Mo from ^{302}122. The half-lives of these cluster emissions are compared or even less than the α-decay half-lives. The above clusters and their residual daughter nuclei have proton and/or neutron numbers correspond to magic or near magic numbers.

[1] K. Siwek-Wilczyńska, T. Cap, and M. Kowal, Phys. Rev. C **99**, 054603 (2019).
[2] M. Ismail and A. Adel, J. Phys. G: Nucl. Part. Phys. **46**, 075105 (2019).
[3] J. R. Stone, K. Morita, P. A. M. Guichon, and A. W. Thomas, Phys. Rev. C **100**, 044302 (2019).
[4] Zhishuai Ge, Gen Zhang, Shihui Cheng, Yuling Li, Ning Su, Wuzheng Guo, Yu. S. Tsyganov, and Feng-Shou Zhang, Eur. Phys. J. A **55**, 166 (2019)
[5] N. T. Brewer *et al.*, Phys. Rev. C **98**, 024317 (2018).
[6] V. K. Utyonkov *et al.*, Phys. Rev. C **97**, 014320 (2018).
[7] M. Ismail and A. Adel, Phys. Rev. C **97**, 044301 (2018).
[8] Yu. Ts. Oganessian and K. P. Rykaczewski, Phys. Today **68**(8), 32 (2015).
[9] Yu. Ts. Oganessian and V. K. Utyonkov, Rep. Prog. Phys. **78**, 036301 (2015).
[10] Yu. Ts. Oganessian and V. K. Utyonkov, Nucl. Phys. A **944**, 62 (2015).
[11] Yu. Ts. Oganessian *et al.*, Phys. Rev. Lett. **104**, 142502 (2010).
[12] S. Hofmann and G. Munzenberg, Rev. Mod. Phys. **72**, 733 (2000).
[13] K. Morita *et al.*, J. Phys. Soc. Jpn. **76**, 043201 (2007).
[14] K. Morita *et al.*, J. Phys. Soc. Jpn. **76**, 045001 (2007).
[15] K. Morita *et al.*, J. Phys. Soc. Jpn. **81**, 103201 (2012).
[16] Yu. Ts. Oganessian, J. Phys. G **34**, R165 (2007).
[17] Yu. Ts. Oganessian *et al.*, Phys. Rev. C **74**, 044602 (2006).
[18] S. Hofmann *et al.*, Eur. Phys. J. A **52**, 180 (2016).
[19] C. Xu and Z. Ren, Nucl. Phys. A **753**, 174 (2005).
[20] A. Adel and T. Alharbi, Nucl. Phys. A **975**, 1 (2018).
[21] W. M. Seif and A. Adel, Phys. Rev. C **99**, 044311 (2019).
[22] H. F. Zhang and G. Royer, Phys. Rev. C **76**, 047304 (2007).
[23] D. S. Delion, S. Peltonen, and J. Suhonen, Phys. Rev. C **73**, 014315 (2006).
[24] S. Peltonen, D. S. Delion, and J. Suhonen, Phys. Rev. C **75**, 054301 (2007).
[25] D. N. Poenaru, M. Ivascu, and A. Sandulescu, J. Phys. G: Nucl. Part. Phys. **5**, L169 (1979).
[26] K. P. Santhosh and C. Nithya, At. Data Nucl. Data Tables **119**, 33 (2018).
[27] K. P. Santhosh and C. Nithya, Eur. Phys. J. A **53**, 189 (2017).
[28] K. P. Santhosh and C. Nithya, Phys. Rev. C **96**, 044613 (2017).
[29] K. P. Santhosh and C. Nithya, Phys. Rev. C **95**, 054621 (2017).
[30] K. P. Santhosh and C. Nithya, Phys. Rev. C **94**, 054621 (2016).
[31] K. P. Santhosh and C. Nithya, Eur. Phys. J. A **52**, 371 (2016).
[32] V. E. Viola, Jr. and G. T. Seaborg, J. Inorg. Nucl. Chem. **28**, 741 (1966).
[33] A. Sobiczewski, Z. Patyk, and S. Cwiok, Phys. Lett. B **224**, 1 (1989).
[34] A. I. Budaca, R. Budaca, and I. Silisteanu, Nucl. Phys. A **951**, 60 (2016).
[35] D. N. Poenaru, R. A. Gherghescu, and N. Carjan, Europhys. Lett. **77**, 62001 (2007).
[36] G. Royer, J. Phys. G: Nucl. Part. Phys. **26**, 1149 (2000).
[37] M. Horoi, B. A. Brown, and A. Sandulescu, J. Phys. G: Nucl. Part. Phys. **30**, 945 (2004).
[38] C. Qi, F. R. Xu, R. J. Liotta, and R. Wyss, Phys. Rev. Lett. **103**, 072501 (2009).
[39] G. Saxena, M. Kumawat, S. Somorendro Singh, and M. Aggarwal, Int. J. Mod. Phys. E **28**, 1950008 (2019).
[40] H. C. Manjunatha, Nucl. Phys. A **945**, 42 (2016).
[41] K. P. Santhosh, B. Priyanka, and C. Nithya, Nucl. Phys. A **955**, 156 (2016).
[42] Y. Qian and Z. Ren, Phys. Rev. C **90**, 064308 (2014).
[43] N. Wang, M. Liu, X. Z. Wu, and J. Meng, Phys. Lett. B **734**, 215 (2014); http://www.imqmd.com/mass/.
[44] S. M. S. Ahmed, R. Yahaya, S. Radiman, and M. S. Yasir, J. Phys. G: Nucl. Part. Phys. **40**, 065105 (2013).
[45] D. Deng, Z. Ren, D. Ni, and Y. Qian, J. Phys. G: Nucl. Part. Phys. **42**, 075106 (2015).
[46] D. Deng and Z. Ren, Phys. Rev. C **93**, 044326 (2016).
[47] S. M. S. Ahmed, Nucl. Phys. A **962**, 103 (2017).
[48] D. Ni, Z. Ren, T. Dong, and C. Xu, Phys. Rev. C **78**, 044310 (2008).
[49] B. Buck, J. C. Johnston, A. C. Merchant, and S. M. Perez, Phys. Rev. C **53**, 2841 (1996).
[50] M. Ismail, A. Y. Ellithi, M. M. Botros, and A. Adel, Phys. Rev. C **81**, 024602 (2010).
[51] A. Adel and T. Alharbi, Phys. Rev. C **92**, 014619 (2015).
[52] N. G. Kelkar and H. M. Castaneda, Phys. Rev. C **76**, 064605 (2007).
[53] R. E. Langer, Phys. Rev. **51**, 669 (1937).
[54] G. R. Satchler and W. G. Love, Phys. Rep. **55**, 183 (1979).
[55] Dao T. Khoa, Phys. Rev. C **63**, 034007 (2001).
[56] N. Anantaraman, H. Toki, and G. F. Bertsch, Nucl. Phys. A **398**, 269 (1983).
[57] C. Xu, Z. Ren, and Y. Guo, Phys. Rev. C **78**, 044329 (2008).
[58] K. Wildermuth and Y. C. Tang, *A Unified Theory of the Nucleus* (Academic, New York, 1977).
[59] Y. Qian, Z. Ren, and D. Ni, Phys. Rev. C **94**, 024315 (2016).
[60] D. Ni and Z. Ren, Phys. Rev. C **82**, 024311 (2010).
[61] A. Adel and T. Alharbi, Nucl. Phys. A **958**, 187 (2017).
[62] M. Ismail, W. M. Seif, and A. Abdurrahman, Phys. Rev. C **94**, 024316 (2016).
[63] W. M. Seif, M. Ismail, A. I. Refaie, and Laila H. Amer, J. Phys. G: Nucl. Part. Phys. **43**, 075101 (2016).
[64] Y. Qian and Z. Ren, Phys. Rev. C **84**, 064307 (2011).
[65] J. C. Pei, F. R. Xu, Z. J. Lin, and E. G. Zhao, Phys. Rev. C **76**, 044326 (2007).
[66] D. Ni and Z. Ren, Nucl. Phys. A **828**, 348 (2009).
[67] B. Buck, A. C. Merchant, and S. M. Perez, Phys. Rev. C **45**, 2247 (1992).
[68] B. Buck, A. C. Merchant, and S. M. Perez, Phys. Rev. C **51**, 559 (1995).
[69] T. T. Ibrahim, A. C. Merchant, S. M. Perez, and B. Buck, Phys. Rev. C **99**, 064332 (2019).
[70] F. Hoyler, P. Mohr, and G. Staudt, Phys. Rev. C **50**, 2631 (1994).
[71] D. Bai and Z. Ren, Eur. Phys. J. A **54**, 220 (2018).
[72] W. M. Seif, A. M. H. Abdelhady, and A. Adel, J. Phys. G: Nucl. Part. Phys. **45**, 115101 (2018).
[73] D. Deng, Z. Ren, and N. Wang, Phys. Lett. B **795**, 554 (2019).
[74] W. M. Seif, M. M. Botros, and A. I. Refaie, Phys. Rev. C **92**, 044302 (2015).
[75] M. Ismail, A. Y. Ellithi, A. Adel, and H. Anwer, J. Phys. G: Nucl. Part. Phys. **43**, 015101 (2016).
[76] M. Ismail, A. Y. Ellithi, A. Adel, and H. Anwer, Chin. Phys. C **40**, 124102 (2016).

[77] J. H. Hamilton, S. Hofmann, and Y. T. Oganessian, J. Phys.: Conf. Ser. **580**, 012019 (2015).
[78] D. S. Delion, Phys. Rev. C **80**, 024310 (2009).
[79] D. N. Poenaru and R. A. Gherghescu, Phys. Rev. C **97**, 044621 (2018).
[80] D. N. Poenaru, H. Stöcker, and R. A. Gherghescu, Eur. Phys. J. A **54**, 14 (2018).
[81] Y. L. Zhang and Y. Z. Wang, Phys. Rev. C **97**, 014318 (2018).
[82] M. Bender, K. Rutz, P.-G. Reinhard, J. A. Maruhn, and W. Greiner, Phys. Rev. C **60**, 034304 (1999).